

A latest fluoride with excellent structural stiffness for ultra-efficient photoluminescence and specific four-peak emission temperature sensing

*Kejie Li^a, Mengmeng Dai^a, Zuoling Fu *^a, Zhiying Wang^a, Hanyu Xu^a and Rong Wang^a*

Coherent Light and Atomic and Molecular Spectroscopy Laboratory, Key Laboratory of Physics and Technology for Advanced Batteries, Jilin University, Changchun 130012, China. E-mail: zlfu@jlu.edu.cn (Z. L. Fu)

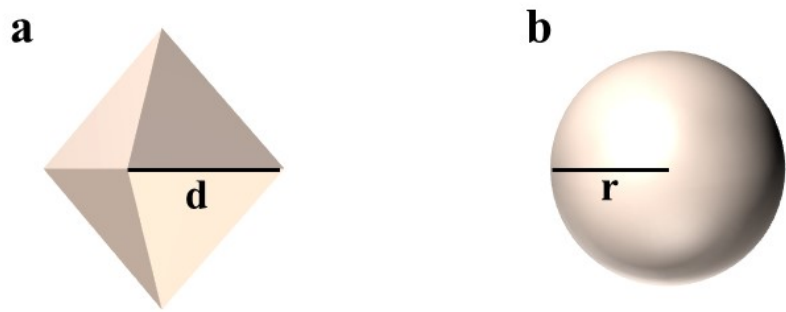


Figure S1 (a) the octahedral cones with edge length d . (b) traditional sphere with radius r .

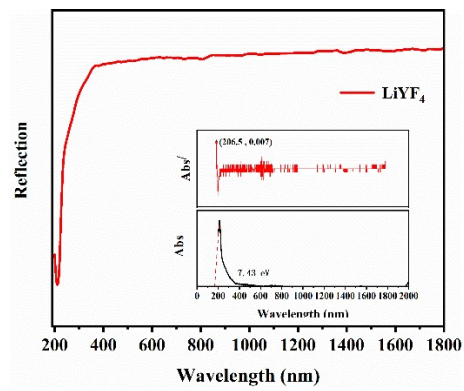


Figure S2 Diffuse reflectance spectrum and band gap calculation.

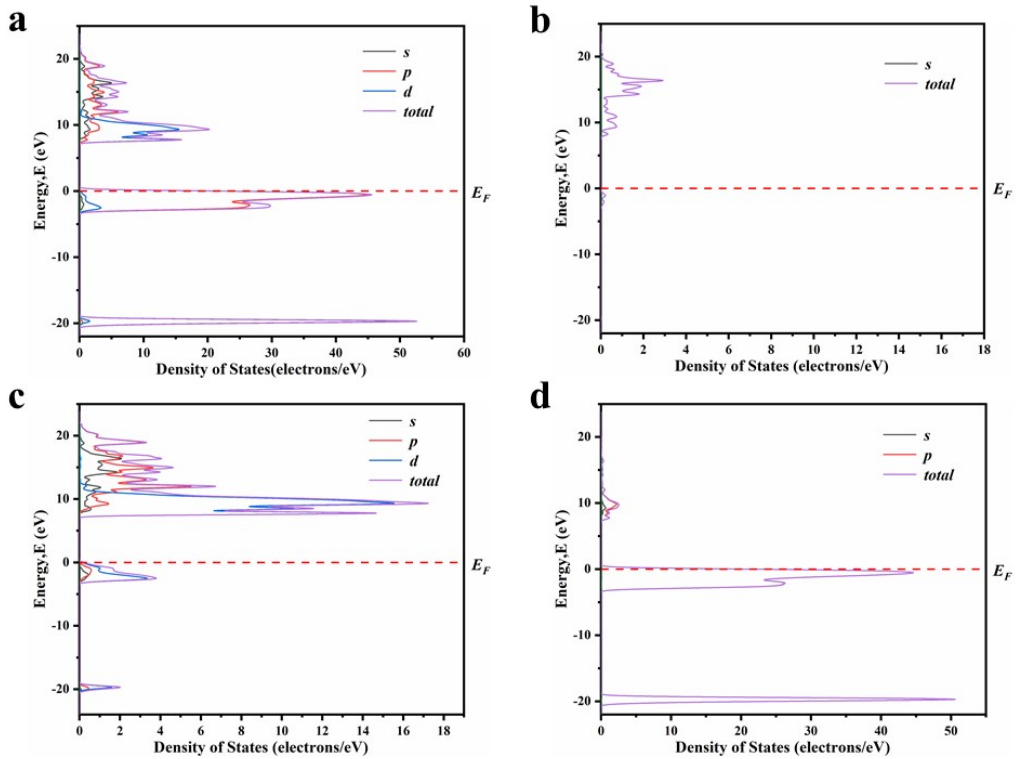


Figure S3 Calculated total DOS and atom-resolved PDOS of LiYF_4 : (a) total; (b) Li; (c) Y; (d) F.

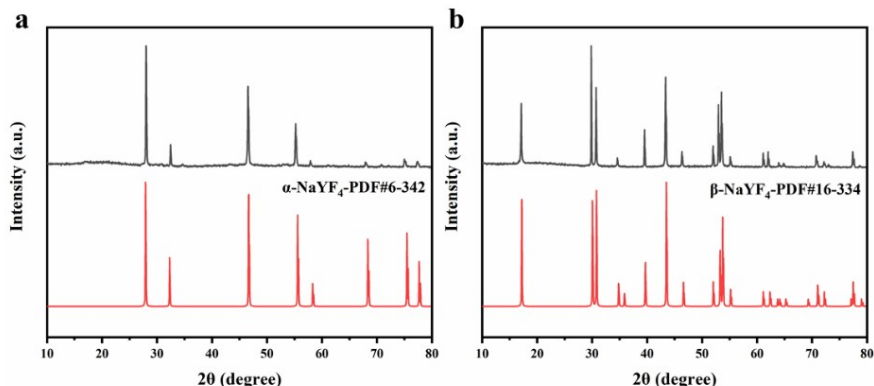


Figure S4 The XRD patterns of $\alpha\text{-NaYF}_4$ (a) and $\beta\text{-NaYF}_4$ (b).

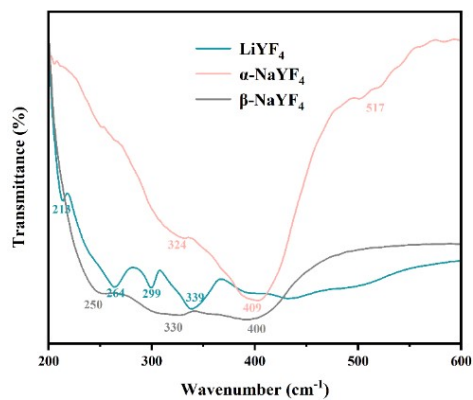


Figure S5 FTIR spectra of LiYF_4 , $\alpha\text{-NaYF}_4$ and $\beta\text{-NaYF}_4$.

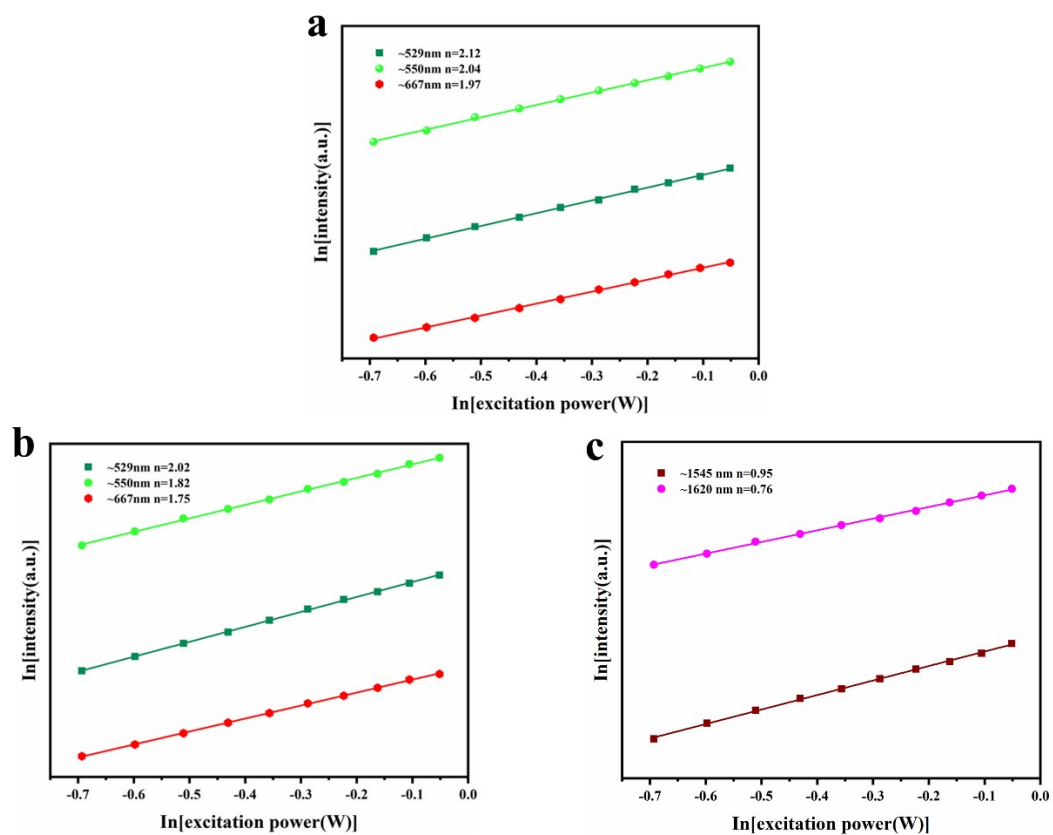


Figure S6 The relationship between $\ln(I)$ and $\ln(P)$ for $\text{LiYF}_4\text{:1\%Er}^{3+}$ under 980 nm (a) and 808 nm (b) excitation in the visible region and near infrared regions (c).

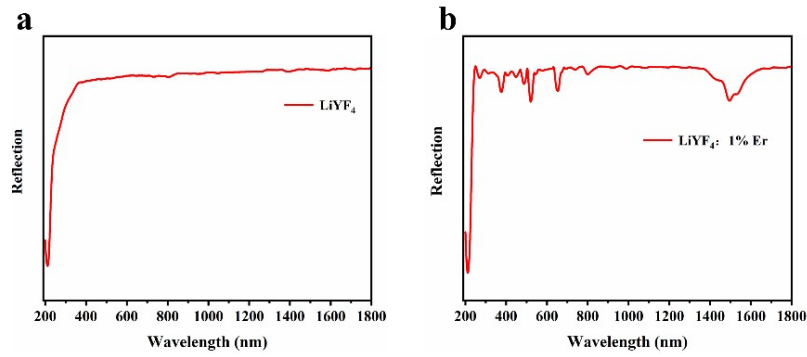


Figure S7 Diffuse reflectance spectrum of LiYF₄ host (a) and LiYF₄:1%Er (b).

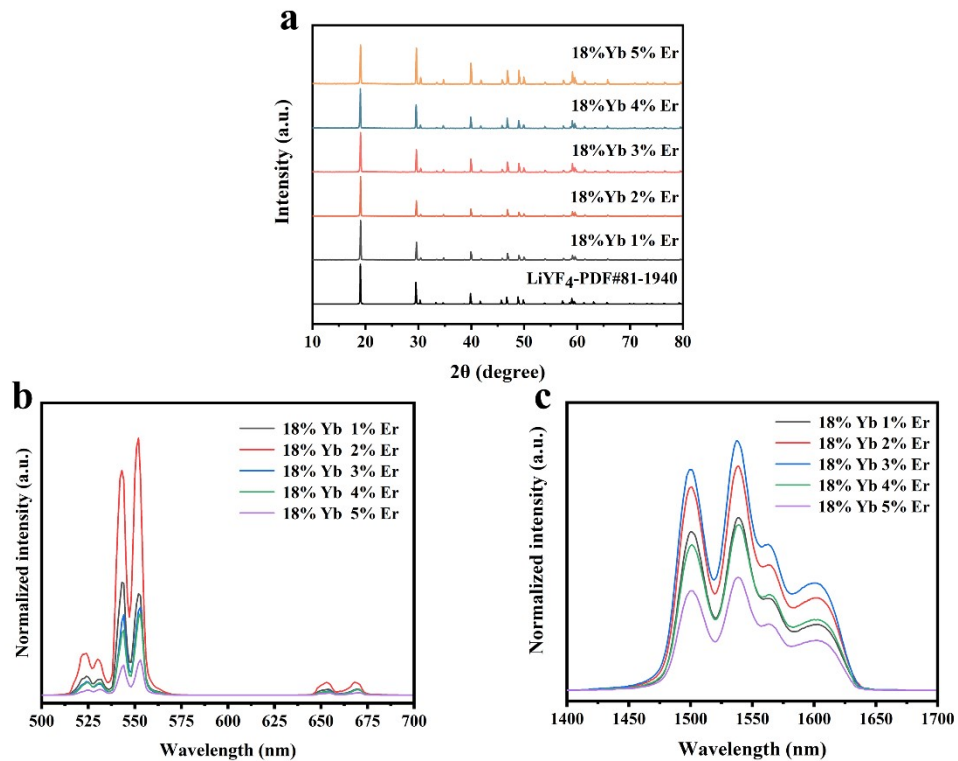


Figure S8 (a) The XRD patterns of LiYF₄:18%Yb³⁺, x%Er³⁺ (x=1, 2, 3, 4, 5) with the standard XRD data of LiYF4 (DPF 81–1940). (b) Visible PL spectra and (c) NIR PL spectra of the LiYF₄:18%Yb³⁺, x%Er³⁺ (x=1, 2, 3, 4, 5) under 980 nm excitation.

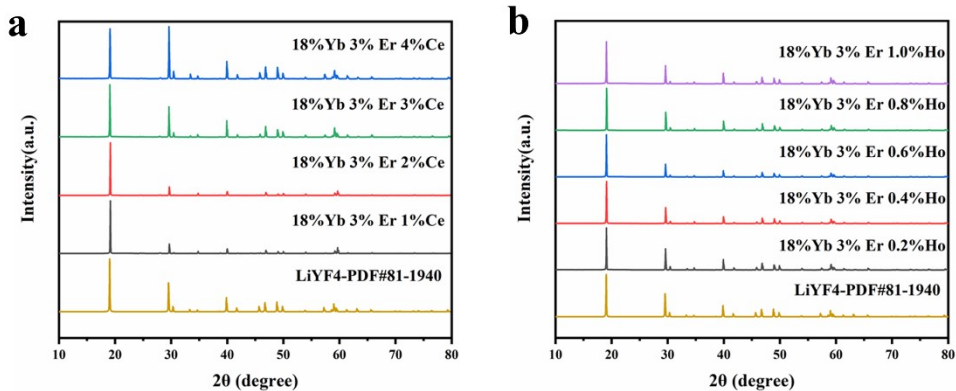


Figure S9 (a) The XRD patterns of LiYF_4 : $18\% \text{Yb}^{3+}$, $3\% \text{Er}^{3+}$, $x\% \text{Ce}^{3+}$ ($x=1, 2, 3, 4$) with the standard XRD data of tetragonal phase LiYF_4 (DPF 81–1940). (b) The XRD patterns of LiYF_4 : $18\% \text{Yb}^{3+}$, $3\% \text{Er}^{3+}$, $x\% \text{Ho}^{3+}$ ($x=0.2, 0.4, 0.6, 0.8, 1.0$) with the standard XRD data of tetragonal phase LiYF_4 (DPF 81–1940).

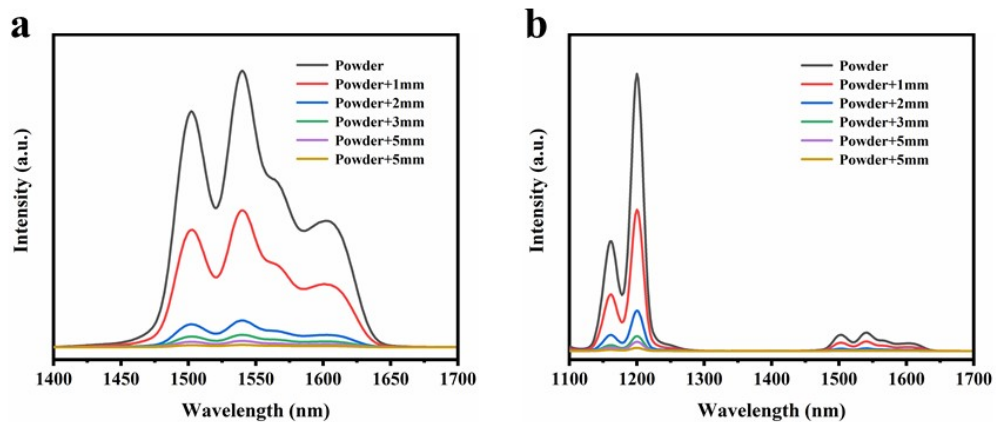


Figure S10 The PL spectra for the LiYF_4 : $18\% \text{Yb}^{3+}$, $3\% \text{Er}^{3+}$, $2\% \text{Ce}^{3+}$ (a) and LiYF_4 : $18\% \text{Yb}^{3+}$, $3\% \text{Er}^{3+}$, $1\% \text{Ho}^{3+}$ (b) with different depths of chicken breast.

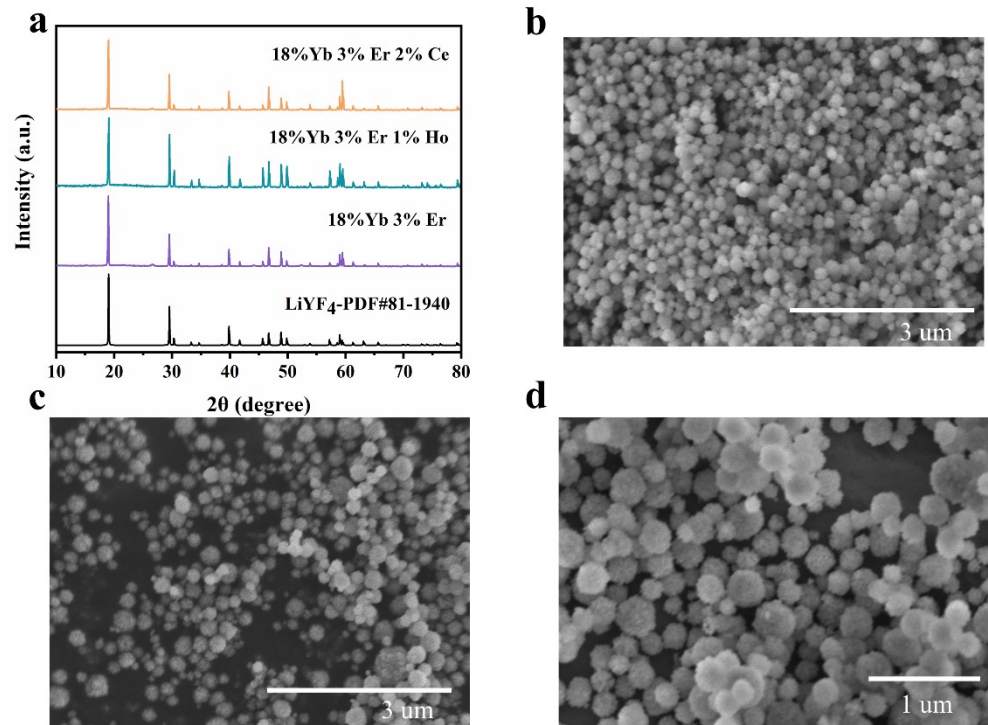


Figure S11 (a) The XRD patterns of LiYF_4 :18% Yb^{3+} , 3% Er^{3+} , LiYF_4 :18% Yb^{3+} , 3% Er^{3+} , 1% Ho^{3+} and LiYF_4 :18% Yb^{3+} , 3% Er^{3+} , 2% Ce^{3+} with the standard XRD data of tetragonal phase LiYF_4 (DPF 81–1940). SEM image of LiYF_4 :18% Yb^{3+} , 3% Er^{3+} (b), LiYF_4 :18% Yb^{3+} , 3% Er^{3+} , 1% Ho^{3+} (c) and LiYF_4 :18% Yb^{3+} , 3% Er^{3+} , 2% Ce^{3+} (d).

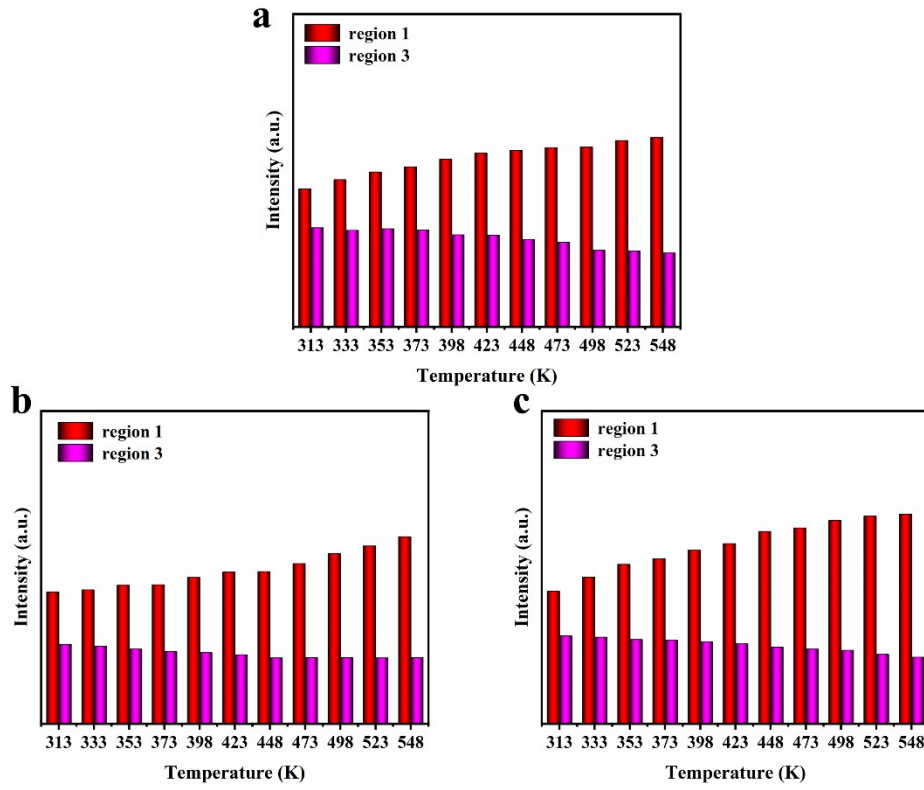


Figure S12 The integrated intensity summarizing of NIR-IIb (region 1.2.3) emission in $\text{LiYF}_4:18\%\text{Yb}^{3+}$, $3\%\text{Er}^{3+}$ (a), $\text{LiYF}_4:18\%\text{Yb}^{3+}$, $3\%\text{Er}^{3+}$, $0.2\%\text{Ho}^{3+}$ (b) and $\text{LiYF}_4:18\%\text{Yb}^{3+}$, $3\%\text{Er}^{3+}$, $2\%\text{Ce}^{3+}$ (c) at different temperature;

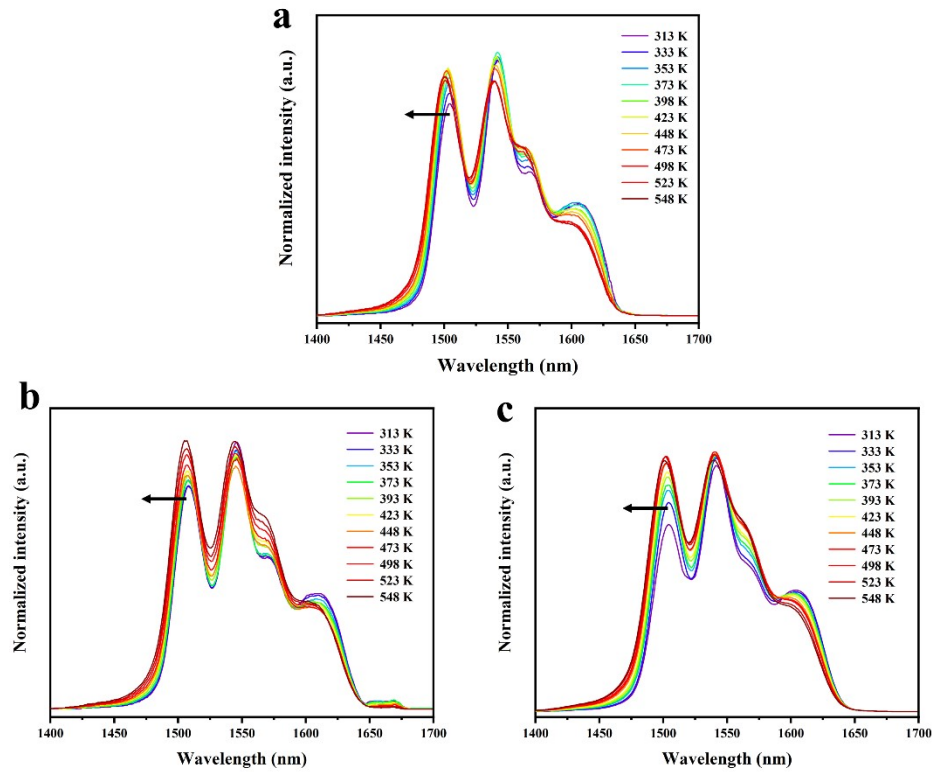


Figure S13 Temperature-dependent NIR-IIb emission spectra of LiYF₄:18% Yb³⁺, 3%Er³⁺ (a), LiYF₄:18%Yb³⁺, 3%Er³⁺, 0.2%Ho³⁺ (b) and LiYF₄:18%Yb³⁺, 3%Er³⁺, 2%Ce³⁺ (c)

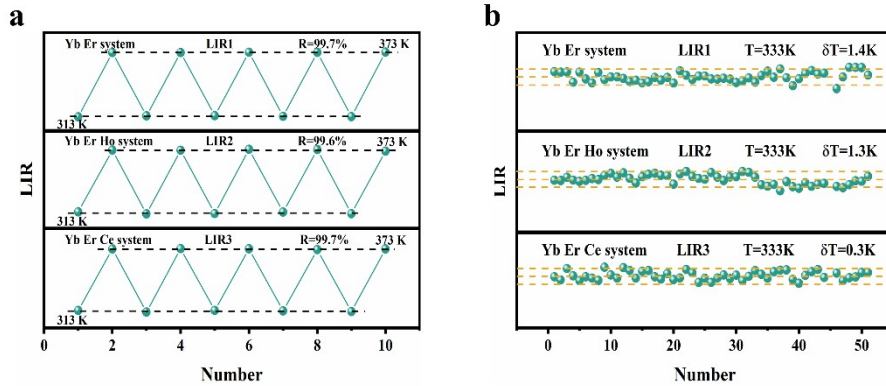


Figure S14 (a) LIR repeatability in 5 heating-cooling cycles. (b) LIR values were measured 50 times continuously at 333 K.

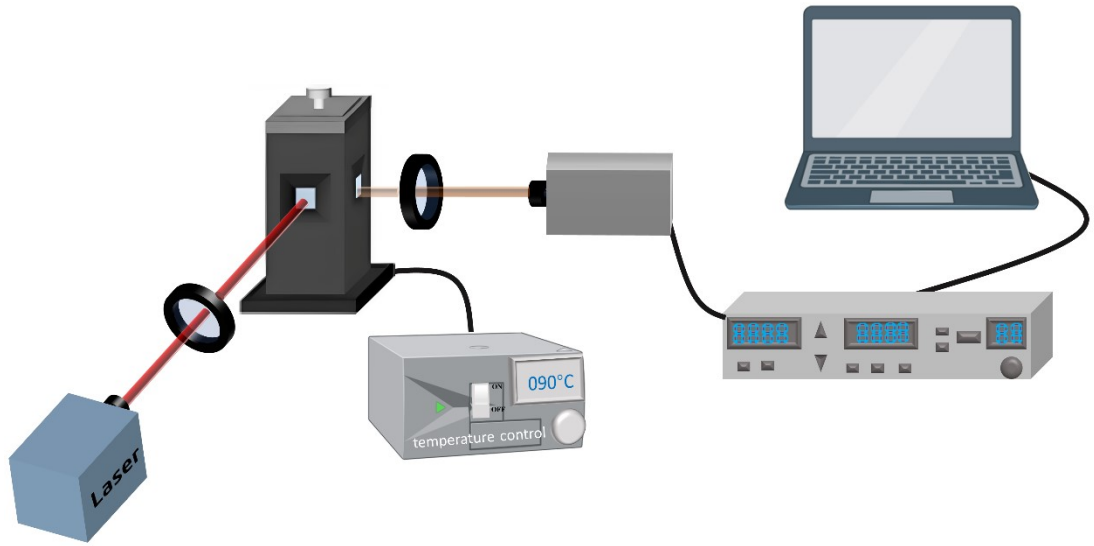


Figure S15 Schematic diagram of the experimental equipment for temperature sensing measurements.

Table S1:

The decomposition of each J in the C_4 point group (Γ_j^\pm is the irreducible representation of $D_j^\pm, (\overline{\Gamma_i + \Gamma_j})$ represents two one-dimensional irreducible representations):

D_0^\pm	Γ_1
D_1^\pm	$\Gamma_1 + (\overline{\Gamma_3 + \Gamma_4})$
D_2^\pm	$\Gamma_1 + 2\Gamma_2 + (\overline{\Gamma_3 + \Gamma_4})$
D_3^\pm	$\Gamma_1 + 2\Gamma_2 + 2(\overline{\Gamma_3 + \Gamma_4})$
D_4^\pm	$3\Gamma_1 + 2\Gamma_2 + 2(\overline{\Gamma_3 + \Gamma_4})$
D_5^\pm	$3\Gamma_1 + 2\Gamma_2 + 3(\overline{\Gamma_3 + \Gamma_4})$
D_6^\pm	$3\Gamma_1 + 4\Gamma_2 + 3(\overline{\Gamma_3 + \Gamma_4})$
D_7^\pm	$3\Gamma_1 + 4\Gamma_2 + 4(\overline{\Gamma_3 + \Gamma_4})$
D_8^\pm	$5\Gamma_1 + 4\Gamma_2 + 4(\overline{\Gamma_3 + \Gamma_4})$
$D_{1/2}^\pm$	$(\overline{\Gamma_5 + \Gamma_6})$

D _{3/2} [±]	($\overline{\Gamma_5 + \Gamma_6}$) ₊ ($\overline{\Gamma_7 + \Gamma_8}$)
D _{5/2} [±]	($\overline{\Gamma_5 + \Gamma_6}$) ₊ 2($\overline{\Gamma_7 + \Gamma_8}$)
D _{7/2} [±]	2($\overline{\Gamma_5 + \Gamma_6}$) ₊ 2($\overline{\Gamma_7 + \Gamma_8}$)
D _{9/2} [±]	3($\overline{\Gamma_5 + \Gamma_6}$) ₊ 2($\overline{\Gamma_7 + \Gamma_8}$)
D _{11/2} [±]	3($\overline{\Gamma_5 + \Gamma_6}$) ₊ 3($\overline{\Gamma_7 + \Gamma_8}$)
D _{13/2} [±]	3($\overline{\Gamma_5 + \Gamma_6}$) ₊ 4($\overline{\Gamma_7 + \Gamma_8}$)
D _{15/2} [±]	4($\overline{\Gamma_5 + \Gamma_6}$) ₊ 4($\overline{\Gamma_7 + \Gamma_8}$)
D _{17/2} [±]	5($\overline{\Gamma_5 + \Gamma_6}$) ₊ 4($\overline{\Gamma_7 + \Gamma_8}$)

Compatibility relationship between group C_{4h} and group C₄:

C_{4h}	Γ_1^+	Γ_2^+	Γ_3^+	Γ_4^+	Γ_1^-	Γ_2^-	Γ_3^-	Γ_4^-	Γ_5^+	Γ_6^+	Γ_7^+	Γ_8^+	Γ_5^-	Γ_6^-	Γ_7^-	Γ_8^-
C_4	Γ_1	Γ_2	Γ_3	Γ_4	Γ_1	Γ_2	Γ_3	Γ_4	Γ_5	Γ_6	Γ_7	Γ_8	Γ_5	Γ_6	Γ_7	Γ_8

Number of energy level splits of J energy levels in the point group: